INSPECTION OF SPECULAR SURFACES USING OPTIMIZED M-CHANNEL WAVELETS

Tan-Toan Le[*†], *Mathias Ziebarth*[*‡], *Thomas Greiner*[†], *Michael Heizmann*[§]

[†] Pforzheim University, Institute for Applied Research, Tiefenbronnerstr. 65, 75175 Pforzheim, Germany
[‡] Karlsruhe Institute of Technology, Institute for Anthropomatics, Adenauerring 4, 76131 Karlsruhe, Germany
[§] Fraunhofer IOSB, Fraunhoferstr. 1, 76131 Karlsruhe, Germany

ABSTRACT

Despite its age the inspection of specular surfaces is still a topic of ongoing research. While sensory approaches to inspect such surfaces based on deflectometry are increasingly used in practice, the evaluation techniques using the acquired signals (images and reconstruction results) are often not sufficient. This work addresses the challenge of detecting defects with different characteristics on specular surfaces by using robust multiscale detection and classification. In order to process the signals obtained by deflectometry efficiently in all relevant scales, a method for generating an optimized biorthogonal wavelet filter bank with strong correlation to any number of anomaly classes is proposed. The filter bank is optimized for each defect class to obtain a sparse scale space representation. In addition a Bayesian classification approach is presented to classify defects like dents and pimples directly in the scale space.

Index Terms— Wavelet-Transform, Optimized filters, Surface topography, Automatic optical inspection

1. INTRODUCTION

We present a new method to evaluate measurements of specular surfaces obtained using deflectometric methods. The main idea is based on the decomposition of a given signal into different scales with optimized wavelet filter banks. The wavelet coefficients from these filter banks are multiscale features which match defects occurring in different sizes. In order to gain better classification results these biorthogonal wavelet filters are optimized for each defect class. Using this optimized filter bank a stationary wavelet transform is used to build a wavelet packet decomposition.

Previous approaches for defect detection on specular surfaces didn't use optimized wavelets. Furthermore no wavelet coefficients were used directly for classification which led to more complicated classifiers. Most of the related work processed single camera images of the surface, while only a few used deflectometric methods. Zhang et al. [1] used the wavelet transform for a smoothing of images taken from a specular surface. The classification was done by a support vector machine (SVM) and based on features taken from spectral measures calculated from a Fourier transform. Fargione et al. [2] used a neural network classifier and some simple features extracted from regions given by an image segmentation. Ghorai et al. [3] compared an SVM and VVRKFA (vector-valued regularized kernel function approximation) classifier with features extracted from a discrete wavelet transform (DWT) with Haar-, Daubechies-, Bior- and Multiwavelets. They divided the image into small square regions and used the DWT to calculate the energy in each scale which in turn was used to classify each region. Jiang and Blunt [4] used a stationary wavelet transform in combination with complex biorthogonal wavelets. This increased redundancy led to a better shift and rotation invariance for surface topographies. Li [5] used a DWT as preprocessing to highlight defects and an SVM to classify regions based on a blob analysis with several extracted features like the area or the compactness of the blobs. Burla et al. [6] and Zheng et al. [7] used genetic algorithms instead of a classifier to adopt the detection to several defect classes. Rosenboom et al. [8] studied the aptitude of several wavelet families for defect detection on deflectometric measurements.

In contrary our focus lies on the features calculated by matched wavelet filter banks. We improve the classification results compared to standard wavelets like biorthogonal spline wavelets as proposed by Cohen et al. [9]. The classifier is intentionally kept simple to understand the process. The paper is organized as follows: in Section 2 and 3 the related work as well as the fundamentals of deflectometry and wavelet theory are introduced. The new method is presented in Section 4 and 5. In Section 6 an application of the new method and classification results are shown. Finally a conclusion is made in Section 7.

2. FUNDAMENTALS OF DEFLECTOMETRY

The challenges when inspecting specular surfaces differ from the challenges on non-reflective surfaces. First of all it's not possible to project any patterns onto the surface and observe them directly. Deflectometric methods are applicable because they exploit the specularity of the surface. The objective of

[*]This work was financed by Baden-Württemberg Stiftung, Germany.

the further evaluation depends on the application. If the objective is to find functional or aesthetic defects, the function of the specular object or the perception of a user respectively has to be considered. For these applications the optical aberrations caused by the surface curvature are more important than the absolute coordinate of each point on the surface. Due to the measurement principle of deflectometry it is especially sensitive to the surface curvature and therefore better suited for those problems. The measurement system consists of a camera with image plane I, a specular surface S and a screen L arranged in a triangular setup. On the screen sinus patterns in horizontal and vertical directions for phase shifting methods are displayed. The camera observes a distorted pattern of the screen over the specular surface. By observing a sequence of patterns, viewing rays from the camera plane P_I can be uniquely assigned to points on the screen P_L:

$$l : P_I \mapsto P_L,\ l[u,v] = (x_L, y_L). \tag{1}$$

This mapping l is called deflectometric registration. Without knowing the distance between the camera and the surface it is impossible to unambiguously reconstruct the surface from the deflectometric registration. Balzer [10] showed two approaches to obtain additional regularizing information of the surface that lead to a unique reconstruction. An overview of several regularizing methods for deflectometry is given by Werling et al. [11]. In the following, we assume that a surface $S(m,n)$ is obtained as result of the deflectometric reconstruction:

$$S(m,n) = z, \text{ with } (m,n) \in \mathbb{N}^2,\ z \in \mathbb{R}. \tag{2}$$

While many different defects can appear on the surface, most of them have a characteristic shape. The size of defects ranges from very small to large, but their shape remains for each class. For this reason wavelets should be an appropiate method to detect and classify these defects.

3. WAVELETS AND OPTIMIZED WAVELETS

3.1. Wavelet transform and filter bank

For a given signal $s(x)$ and a set of band-pass wavelet functions $\psi^i(x)$, $i \in \mathbb{N}$ and low-pass scaling functions $\phi^i(x)$, $i \in \mathbb{N}$, a continuous wavelet transform will analyze the signal with the corresponding basis, which is established by translation k and dilation j of the wavelets $\{\psi_{j,k}(x) \mid j \in \mathbb{R}^+,\ k \in \mathbb{R}\}$ and scaling functions $\{\phi_{j,k}(x) \mid j \in \mathbb{R}^+,\ k \in \mathbb{R}\}$. The detail coefficients of the wavelet transform are calculated as

$$d^i_{j,k} = \langle s(x), \psi^i_{j,k}(x)\rangle, \psi^i_{j,k}(x) = 2^{-j/2}\psi^i(2^{-j}x - k) \tag{3}$$

and the approximation coefficients are calculated as

$$a^i_{j,k} = \langle s(x), \phi^i_{j,k}(x)\rangle, \phi^i_{j,k}(x) = 2^{-j/2}\phi^i(2^{-j}x - k). \tag{4}$$

With respect to regularity conditions, continuous wavelets and scaling functions can be converted to a discrete filter bank [12].

3.2. Optimizing wavelets for classification purposes

The idea of optimizing the wavelet basis for a given problem and then classifying the coefficients has been discussed by other authors before. Szu et al. [13] optimized the dilation and translation parameters for the Morlet wavelet, which were used by an artificial neuronal network classifier. For feature extraction from near-infrared data Mallet et al. [14] optimized the wavelet filter coefficients by maximizing a chosen discriminant criterion between classes with respect to conditions for orthogonality and regularity of filters. Maitrot et al. [15] applied two new methods to parametrize the mother wavelet: one for orthogonal and one for semiorthogonal wavelets. In the case of orthogonal wavelets only the coefficients of the scaling filter h need to be defined. In the case of semiorthogonal wavelets, a new wavelet ψ is optimized as a linear combination of a given wavelet ψ^0 with an admissible sequence p: $\psi = p * \psi^0$. Quellec et al. [16] used the popular lifting scheme framework introduced by Sweldens [17] to find the optimized wavelet basis for content-based image retrieval in a medical database. With matched wavelet bases a signature characterizing the distribution of wavelet coefficients in each subband of the decomposition was built. These signatures were used for image classification.

The procedure for designing a biorthogonal wavelet filter bank presented in this paper is mainly based on the concept introduced by Greiner [18]. He showed a method for generating a texture-matched FIR-filter bank for both orthogonal and biorthogonal filter banks. In contrast to Greiner we use the stationary wavelet transform introduced by Holschneider et al. [19] which yields a better localization of defects. From the wavelet decomposing tree, coefficients on different nodes are chosen as feature for the classifier. This concept differs from the optimization methods presented above.

4. OPTIMIZING WAVELETS FOR SURFACE DATA

The main idea of this optimization method is to approximate each defect class and use it as basis to design a wavelet filter bank consisting of a matched band-pass filter for each class and the associated biorthogonal low-pass filter. First of all for each defect class C_i on a given specular surface S a one-dimensional curve to describe an average defect is extracted. After normalization to $\sqrt{2}$, the N sampling points of the curve define a filter $\boldsymbol{h}_0$ with length N.

4.1. Conditions for perfect reconstruction

The z-transform $\boldsymbol{H}_1(z)$ of filter $\boldsymbol{h}_1$, which is biorthogonal to $\boldsymbol{h}_0$, can be defined based on the condition for perfect reconstruction (PR) of filter banks. An M-channel filter bank consists of M analysis filters $\boldsymbol{H}_t$ as well as M synthesis filters $\boldsymbol{G}_t$. A signal $s(n)$ can be analyzed by the filters $\boldsymbol{H}_t$ to create decomposition coefficients. With the filters $\boldsymbol{G}_t$ these coefficients can be used to construct a signal $\hat{s}(n)$. In case of $s(n) = z^{-n_0} * \hat{s}(n)$ the filter bank is called a *filter bank allowing perfect reconstruction* [20]. Using an M-channel filter bank, an analyzed signal will be perfectly reconstructed from its wavelet coefficients if the determinant $\Delta_P(z)$ of the polyphase-matrix $P(z)$ of the filters $\boldsymbol{h}_t$ $(t = 0, .., M-1)$ consists of only a single term z^{-n_0} [18]. $P(z)$ has the form:

$$P_{ij}(z) = z^{-j} H_{ij}(z^M). \tag{5}$$

Here $H_{ij}(z^M)$ is the jth polyphase component of the ith filter [20]. Its determinant $\Delta_P(z)$ can be calculated as:

$$\Delta_P(z) = c_0 z^{-M\frac{M-1}{2}} + \ldots + c_{N-M} z^{-[MN - M\frac{M+1}{2}]}, \tag{6}$$

with the constants c_m, $m = 0, \ldots, N-M$.

4.2. Quality criteria

For an M-channel filter bank consisting of $M-1$ filters $\boldsymbol{h}_t$, $(t = 0, \ldots, M-2)$, a filter $\boldsymbol{h}_{M-1}$ which is biorthogonal to all $\boldsymbol{h}_t$ is constructed. In order to match the biorthogonal wavelet filter bank to a given defect class, a quality criterion Q is defined as Euclidean distance between the filter $\boldsymbol{h}_i$ of the defect class C_i and the filter to be constructed $\boldsymbol{h}_{M-1}$:

$$Q = \|\boldsymbol{h}_i - \boldsymbol{h}_{M-1}\|^2. \tag{7}$$

By maximizing the quality criterion Q the filter $\boldsymbol{h}_{M-1}$ will be optimized to be as different from the given defect class as possible. Due to the condition for PR above all the constants c_j in (6) except one need to be set to zero. The constants c_j are weighted sums of coefficients of the filter $\boldsymbol{h}_{M-1}$ to be constructed:

$$c_j = \sum_{n=0}^{N-1} a_{mn} \boldsymbol{h}_{M-1}(n). \tag{8}$$

The construction of $\boldsymbol{h}_{M-1}$ can thus be considered as optimizing quality criterion Q under the constraint that the condition for PR is fulfilled. As a linear system, the set of $(N-M)$ equations $c_j \stackrel{!}{=} 0$, which contain the filter coefficients $\boldsymbol{h}_{M-1}(n)$, $(n = 0, \ldots, N-1)$, is optimized with respect to Q. In order to solve this optimization problem a Lagrange function with Lagrange multiplier $\boldsymbol{\lambda}$ is defined as:

$$L(\boldsymbol{h}_{M-1}, \boldsymbol{\lambda}) = \frac{1}{2} Q - \boldsymbol{\lambda}^T [\boldsymbol{A}\boldsymbol{h}_{M-1} - \boldsymbol{0}]. \tag{9}$$

The optimum can be found by solving the derivation equations:

$$\nabla_{\boldsymbol{h}_{M-1}, \boldsymbol{\lambda}} L(\boldsymbol{h}_{M-1}, \boldsymbol{\lambda}) \stackrel{!}{=} 0. \tag{10}$$

This way the coefficients of filter $\boldsymbol{h}_{M-1}$, which are biorthogonal to given filters $\boldsymbol{h}_t$ $(t = 0, ..., M-2)$, are defined.

After the coefficients of all filters $\boldsymbol{h}_t$ are defined, a filter bank for the stationary wavelet transform is created based on these filters. Each surface is analyzed with a filter bank which results in a wavelet packet tree. Each coefficient node d_k is numbered consecutively as shown in Figure 1 for the case of a 3-channel filter bank in 2 scales.

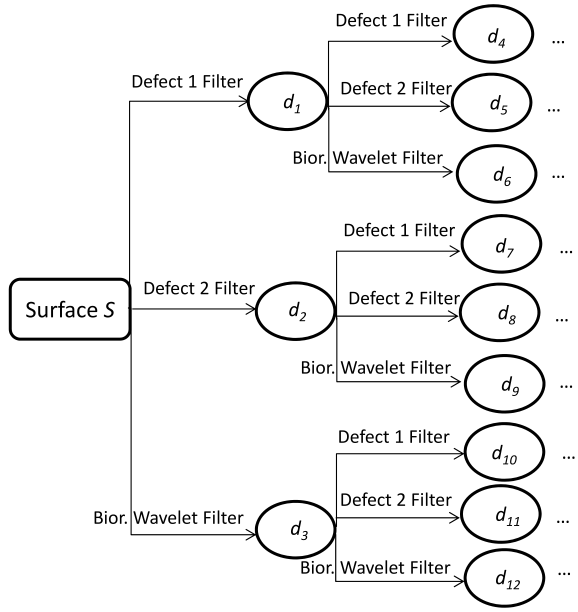

Fig. 1. Wavelet packet tree in case of a 3-channel filter bank.

5. CLASSIFICATION OF DEFECTS

To classify each point on the surface a method to extract features and a classifier are needed. The feature set $\mathbf{d}$ for a point (m, n) on the surface S is given by selected coefficients at the same point $d_k(m, n)$ from the nodes d_k of the wavelet packet tree. The coefficients are calculated as described above with M filters in up to l scales.

$$\mathbf{d}(m, n) \subseteq \{d_1(m, n), \ldots, d_{M+M^2+\ldots+M^l}(m, n)\}. \tag{11}$$

For the classification a maximum a posteriori decision is made for each point on the surface separately. By defining the parameter vectors $\boldsymbol{\mu}_i$ and $\boldsymbol{\sigma}_i$ as mean and standard deviation of each coefficient in class C_i for all selected nodes, the probability for a feature vector $\mathbf{d}$ belonging to class C_i is determined by Bayes' rule:

$$p(\boldsymbol{\mu}_i, \boldsymbol{\sigma}_i | \mathbf{d}) = \frac{p(\mathbf{d}|\boldsymbol{\mu}_i, \boldsymbol{\sigma}_i)\, p(\boldsymbol{\mu}_i, \boldsymbol{\sigma}_i)}{p(\mathbf{d})}. \tag{12}$$

Tests have shown that the coefficients can often be assumed as Laplace distributed. In consequence the likelihood for class C_i is modelled as product of univariate Laplace distributions:

$$p(\mathbf{d}|\boldsymbol{\mu}_i, \boldsymbol{\sigma}_i) = \prod_k \frac{1}{\sigma_{i,k}\sqrt{2\pi}} \exp\left(-\frac{1}{2}\frac{|d_k - \mu_{i,k}|}{\sigma_{i,k}^2}\right). \tag{13}$$

The parameters $\boldsymbol{\mu}_i$ and $\boldsymbol{\sigma}_i$ for each class C_i are learned with a training set for each class. The prior is chosen as being uniformly distributed, but this could be changed in practice.

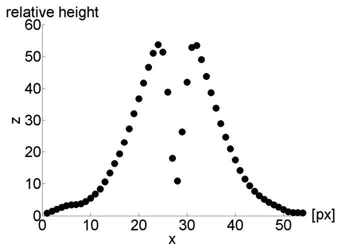

Fig. 2. Curve of a dent.

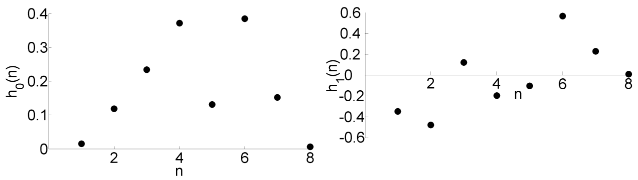

(a) dent filter (b) biorthogonal dent filter

Fig. 3. Impulse responses of a dent filter.

6. RESULTS

In order to demonstrate how this new method improves the classification rate, deflectometry data from several curved lacquered surfaces with many large dents and small pimples were analyzed. Since dents and pimples are the most common defects on our lacquered surfaces, the experiment was performed using these two classes. Additionally each surface has uneven formations, called orange peel, which results in a high measurement noise and complicates the detection of defects. In Figure 2 the 2D-curve of a dent taken from a specular surface is shown. 8 sampling points were extracted from the curve and then normalized to $\sqrt{2}$ to build a filter. The impulse response of this filter together with the associated biorthogonal wavelet filter, which was found by the optimization method in Section 4, are shown in Figure 3.

The classification procedure described in Section 5 was first performed with a biorthogonal spline wavelet 3.5. The results given in Table 1 show moderate accuracy (percentage of true classifications to all classifications) for the class *dent* C_d and a low accuracy for the class *pimple* C_p, where only a third of all defects was classified correctly. The reason for this may be the different shape of pimples on the surface and the shape of biorthogonal wavelet. Based on the filter design method presented in Section 4, four filter banks were created:

- Two systems with 2 channels each: a 2-channel system of the dent filter and its associated biorthogonal filter, as well as a 2-channel system of the pimple filter and its associated biorthogonal wavelet filter,

- A 3-channel system for the case of a filter, which is biorthogonal to both dents and pimples,

			accuracy			
			surface one		**surface two**	
standard wavelet			C_d	C_p	C_d	C_p
biorthogonal spline wavelet 3.5			88%	35%	96%	94%
M	**adapted**	**selected nodes**	C_d	C_p	C_d	C_p
2	C_d	1	90%	73%	99%	96%
2	C_d	1, 3	87%	75%	99%	96%
2	C_d	1, 3, 4	86%	75%	99%	95%
2	C_p	1	67%	78%	99%	97%
3	C_d, C_p	1, 2	86%	78%	99%	96%
3	C_d, C_p	1, 2, 4, 5, 7, 8	83%	78%	99%	95%
4	C_d, C_p	1, 2	84%	79%	99%	97%

Table 1. Comparison of the classification accuracy using a standard wavelet and optimized wavelets for our classification method, the classes *dent* C_d and *pimple* C_p and two specular surfaces.

- And a 4-channel system as a combination of the two systems with 2-channels above.

An extract for the accuracy results of each class using the 4 filter bank systems above with chosen coefficients is shown in Table 1. The nodes were numbered as in Figure 1. The results show that a good accuracy can be achieved by using features from the correlating filter of each class together with its associated biorthogonal wavelet filter: on surface one up to 90% for the class *dent* as well as 78% for the class *pimple* were classified correctly. Compared to the classification with the biorthogonal spline wavelet 3.5 there is a strong improvement for the classification of pimples and a slight improvement for the dents on surface one. On surface two the classification results of all wavelets are similar, but the classification of pimples is slightly better using the correlated wavelet.

Using two 2-channel systems for the classification leads to a similar accuracy as using one 3-channel system. The 4-channel system doesn't improve the results, so the 3-channel system should be the best choice for efficiency reasons.

7. CONCLUSION

A novel method for the analysis of deflectometry signals obtained from specular objects was presented. For each defect class a defect filter and an associated biorthogonal filter were constructed from sample points and were used to build a biorthogonal wavelet filter bank. By means of these filter banks different defect classes on specular objects can be classified. The accuracy rates using the optimized wavelets were improved compared to classic biorthogonal wavelets.

8. REFERENCES

[1] X.-W. Zhang, Y.-Q. Ding, Y.-Y. Lv, A.-Y. Shi, and R.-Y. Liang, "A vision inspection system for the surface defects of strongly reflected metal based on multi-class svm," *Expert Systems with Applications*, vol. 38, pp. 5930–5939, 2011.

[2] G.A. Fargione, A.L. Geraci, L. Pennisi, and A. Risitano, "Development of an algorithm for the analysis of surface defects in mechanical elements," in *Proceedings of SPIE International Symposium on Intelligent Systems and Advanced Manufacturing Conference*, 1998.

[3] S. Ghorai, A. Mukherjee, M. Gangadaran, and P. K. Dutta, "Automatic defect detection on hot-rolled flat steel products," *Instrumentation and Measurement, IEEE Transactions on*, vol. PP, pp. 1–10, 2012.

[4] J. Xiangqian and B. Liam, "Third generation wavelet for the extraction of morphological features from micro and nano scalar surfaces," *Wear*, vol. 257, pp. 1235–1240, 2004.

[5] T.-S. Li, "Applying wavelets transform, rough set theory and support vector machine for copper clad laminate defects classification," *Expert Systems with Applications*, vol. 36, pp. 5822–5829, 2009.

[6] A. Burla, T. Haist, W. Lyda, and W. Osten, "Genetic programming applied to automatic algorithm design in multi-scale inspection systems," *Optical Engineering*, vol. 51, pp. 067001–1–067001–13, 2012.

[7] H. Zheng, L.X. Kong, and S. Nahavandi, "Automatic inspection of metallic surface defects using genetic algorithms," *Journal of Materials Processing Technology*, vol. 125–126, pp. 427–433, 2002.

[8] L. Rosenboom, T. Kreis, and W. Jüptner, "Surface description and defect detection by wavelet analysis," *Measurement Science and Technology*, vol. 22, pp. 1–9, 2011.

[9] A. Cohen, I. Daubechies, and J.C. Feauveau, "Biorthogonal bases of compactly supported wavelets," *Communications on pure and applied mathematics*, vol. 45, no. 5, pp. 485–560, 2006.

[10] J. Balzer, *Regularisierung des Deflektometrieproblems – Grundlagen und Anwendung*, Ph.D. thesis, Universität Karlsruhe (TH), 2008.

[11] S. Werling, M. Mai, M. Heizmann, and J. Beyerer, "Inspection of specular and partially specular surfaces," *Metrology and Measurement Systems*, vol. 16, pp. 415–431, 2009.

[12] O. Rioul, "Simple regularity criteria for subdivision schemes," *SIAM Journal on Mathematical Analysis*, vol. 23, no. 6, pp. 1544–1576, 1992.

[13] H.H. Szu, B.A. Telfer, and S.L. Kadambe, "Neural network adaptive wavelets for signal representation and classification," *Optical Engineering*, vol. 31, no. 9, pp. 1907–1916, 1992.

[14] Y. Mallet, D. Coomans, J. Kautsky, and O. De Vel, "Classification using adaptive wavelets for feature extraction," *Pattern Analysis and Machine Intelligence, IEEE Transactions on*, vol. 19, no. 10, pp. 1058–1066, 1997.

[15] A. Maitrot, M.F. Lucas, and C. Doncarli, "Design of wavelets adapted to signals and application," in *Acoustics, Speech, and Signal Processing, 2005. Proceedings.(ICASSP'05). IEEE International Conference on*. IEEE, 2005, vol. 4, pp. iv–617.

[16] G. Quellec, M. Lamard, G. Cazuguel, B. Cochener, C. Roux, et al., "Wavelet optimization for content-based image retrieval in medical databases," *Medical image analysis*, vol. 14, no. 2, pp. 227–241, 2010.

[17] W. Sweldens, "The lifting scheme: A custom-design construction of biorthogonal wavelets," *Applied and Computational Harmonic Analysis*, vol. 3, no. 2, pp. 186, 1996.

[18] T. Greiner, "Orthogonal and biorthogonal texture-matched wavelet filterbanks for hierarchical texture analysis," *Signal processing*, vol. 54, no. 1, pp. 1–22, 1996.

[19] M. Holschneider, R. Kronland-Martinet, J. Morlet, and P. Tchamitchian, "A real-time algorithm for signal analysis with the help of the wavelet transform," *Time-Frequency Methods and Phase Space*, pp. 289–297, 1989.

[20] M. Vetterli, "Filter banks allowing perfect reconstruction," *Signal processing*, vol. 10, no. 3, pp. 219–244, 1986.